Beam Management and Self-healing for mmWave UAV Mesh Networks

Pei Zhou, Xuming Fang, *Senior Member, IEEE,* Yuguang Fang, *Fellow, IEEE,* Rong He, Yan Long, *Member, IEEE* and Gaoyong Huang

***Abstract*—The point-to-point and point-to-multipoint communication features in the IEEE 802.11ay make it possible for unmanned aerial vehicles (UAVs) to form a UAV mesh network (flyMesh). In an 802.11ay based millimeter-wave (mmWave) flyMesh, many challenges are brought by the collaborative interactions of UAVs and the beam misalignment of the directional communication links. This paper studies how to guarantee the robustness of the mmWave flyMesh with respect to beam management and network self-healing. Firstly, to cope with the problem of beam misalignment between UAVs or between the UAV group leader and relay Base Station (rBS)/satellite caused by the movement of UAV(s), we propose a fast beam tracking mechanism. Secondly, in order to solve the problem of link failures due to departures of some UAVs from the group or failures, the self-healing mechanism is proposed to find alternative links to restore the network capability. Finally, to deal with the dynamic group leader changes of UAVs due to mobility, we propose an efficient UAV group leader re-selection mechanism to reduce the overhead of UAV group management. Through performance analysis and simulation, we demonstrate that our proposed mechanisms can effectively address the aforementioned problems and challenges.**

***Index Terms*—unmanned aerial vehicle (UAV), mmWave network, beam management, beam tracking, self-healing.**

I. Introduction

DURING the past decade, the miniaturization and low cost have made unmanned aerial vehicles (UAVs) popular in public. Due to the flexible landing, UAVs are used to support various services, such as data collection from remote and dangerous or inaccessible areas, surveillance and monitoring tasks, light cargo delivery, and especially disaster rescue [1]–[4]. Therefore, there is no doubt that UAVs have tremendous market potential. However, the sustainability, stability, reliability, and coverage of a single UAV have various limitations, and frequent interruptions of services will occur if we frequently use a new UAV to replace the failed one to continue the task. Thus, the collaboration of UAVs by forming a UAV mesh network, namely, flyMesh, has become an interesting research topic [1]–[5]. The inter-connection between different UAVs can achieve a fully connected network of UAVs. Thus, the reliability and coverage of the flyMesh can be guaranteed. For example, in disaster rescue, when some UAVs become damaged or depart from the network, the rest of the UAVs in the flyMesh can quickly reconfigure itself and continue with the mission. Hence, the operations of the entire flyMesh will not be greatly affected.

The acquired data may be transmitted to a relay Base Station (rBS), an airship, or a satellite (for simplicity, we use 'rBS' to represent 'relay Base Station, airship or satellite' throughout this paper) by the UAV group leader, and then the rBS transmits the data to a Control Center. A flyMesh can also provide emergency communication services when necessary [1]–[4], [6]. However, a large amount of spectra will be needed when a huge amount of data is acquired by UAVs to be transmitted between UAVs or between the flyMesh and rBS. Limited by the available spectra in microwave band (e.g., sub-6GHz), it is almost impossible to guarantee ultra-high-speed and real-time transmissions over the flyMesh. Fortunately, there are large available spectra in millimeter-wave (mmWave), which makes it possible for the flyMesh to provide ultra-high-speed transmissions [7]–[10]. However, due to the severe path loss over mmWave band, the communication distance is short. In order to increase the communication distance over mmWave band, beamforming technologies are needed to concentrate the transmit power over a narrow beam to realize directional communications [7]–[10]. Recently, Ge *et al.* proposed an orbital angular momentum spatial modulation (OAM-SM) mmWave communication system in [11], which can achieve longer-range transmissions than the conventional multiple-input multiple-output (MIMO) mmWave communications. Besides, due to the mobility and high altitude of UAVs, it is possible to form line-of-sight (LOS) paths among UAVs to leverage the beamforming technologies in mmWave communications.

In fact, the wireless local area networks (WLANs) based on IEEE 802.11ad [12] and 802.11ay [13] have already tapped on the mmWave (e.g., 60 GHz) to support point-to-point and point-to-multipoint communications. Thus, the beam management mechanisms of the two aforementioned WLANs can be easily adopted into the flyMesh. Therefore, in this paper, we study the flyMesh based on the 802.11ad and 802.11ay.

The work of P. Zhou, X. Fang, R. He, Y. Long and G. Huang was supported in part by NSFC under Grant 61471303, in part by the NSFC Guangdong Joint Foundation under Grant U1501255, in part by Cultivation Program for the Excellent Doctoral Dissertation of Southwest Jiaotong University, in part by NSFC under Grant 61601380 and in part by the Fundamental Research Funds for the Central Universities under Grant 2682016CX132. The work of Y. Fang was supported in part by the U.S. National Science Foundation under Grant CNS-1717736 and Grant CNS-1343356. *(Corresponding author: Xuming Fang.)*

P. Zhou, X. Fang, R. He, Y. Long and G. Huang are with Key Lab of Information Coding & Transmission, Southwest Jiaotong University, Chengdu 610031, China (e-mail: peizhou@my.swjtu.edu.cn; xmfang@swjtu.edu.cn; rhe@swjtu.edu.cn; yanlong@home.swjtu.edu.cn; huanggaoyong@163.com).

Y. Fang is with the Department of Electrical and Computer Engineering, University of Florida, 435 New Engineering Building, PO Box 116130, Gainesville, FL 32611, USA (e-mail: fang@ece.ufl.edu).

However, there are many design challenges when adopting directional communications in mmWave WLANs, particularly in our mmWave flyMesh:

- Considering that the mmWave flyMesh is deployed in the sky, the relative position between UAVs is changing frequently, which requires frequent beam tracking between the UAVs that have established communication links to ensure real-time beam alignment, and thus providing reliable and ultra-high-speed wireless transmissions. Since a UAV's life time is limited by the battery [4], [6], frequent beam training may waste precious data transmission opportunities. Therefore, fast beam tracking methods should be developed in order to effectively harness benefits of the mmWave flyMesh.
- In some specific circumstances and scenarios (e.g., disaster areas, etc.), some UAVs may fail to function normally because the mmWave flyMesh is vulnerable to the impacts of various environmental or physical factors. Significant changes of the whole mmWave flyMesh topology due to the invalidity of individual UAV should be avoided, otherwise almost all UAVs need to redo their beam tracking with their surrounding UAVs. Therefore, efficient network self-healing methods are needed to guarantee the Quality-of-Service (QoS).
- A UAV group leader should be selected as the gateway to connect with the rBS for data transmissions. However, the relative position between the UAV group leader and rBS may change frequently due to the movement of the mmWave flyMesh in the air, and the backhaul link between the UAV group leader and rBS may not provide a high transmission rate due to its poor channel quality [5]. Thus, UAV group leader re-selection is needed to ensure ultra-high-speed backhaul link transmissions.

There exist some works tackling the aforementioned challenges. Wang *et al*. proposed an efficient gateway-selection algorithm and management mechanism for multi-UAV based heterogeneous flying ad hoc networks, based on the observation that the gateways constitute the bottleneck and limit the network's reliable connectivity and stability [1]. Tang *et al.* in [5] proposed a game theoretic approach based on partially overlapping channels assignment to address the problems of dynamic topology and high mobility of nodes in combined UAV and device-to-device (D2D) based networks. Takaishi *et al.* in [14] proposed a virtual cell based resource allocation scheme to solve the wireless-communication conflicts when several unmanned aircraft systems are operated within the neighboring airspace. However, all these research works are based on microwave band while the directional transmissions in mmWave band will bring more challenges. In addition, the large available spectra will make resource (especially the frequency) allocation less significance in mmWave band. For the mmWave based flyMesh, beam management is important to maintain inter-connection between mmWave UAVs. The IEEE 802.11ad and 802.11ay develop a two-phase beam training method as described in our previous works [15]–[17]. An efficient beam tracking scheme was also introduced in [12], [13], where the beam tracking initiator can append training (TRN) units to data frames to perform flexible beam tracking. Although the current relevent methods can address some challenges of the mmWave flyMesh to some extent, these methods have not fully addressed the reliability of the mmWave flyMesh.

In this paper, we investigate beam management, network self-healing and UAV group leader re-selection mechanisms in the mmWave flyMesh based on the 802.11ad/ay. Beam management is the foundation to ensure the robustness of mmWave flyMesh and an efficient beam management mechanism should cope with the beam misalignment due to UAVs' mobility. Network self-healing capability can quickly find a forwarding link to substitute the failed link due to malfunctioned UAV to maintain the stability of the mmWave flyMesh, and the impact on the entire mmWave flyMesh should be minimized due to link failures. For the UAV group leader re-selection problem, it is necessary to limit the number of candidate UAV group leaders and then perform beam training between the candidate UAV group leaders and rBS. The overhead of UAV group leader re-selection should be minimized. In summary, this paper has made the following major contributions:

1) We propose a fast beam tracking mechanism to solve the beam misalignment problem due to the relative mobility between UAVs and between the UAV group leader and rBS. Based on the variations of Signal-to-Interference plus Noise Ratio (SINR) values on the directional beams, we can infer the directions of relative movements. Thus we can limit the region of beam tracking and hence reduce the overhead.
2) We develop a self-healing mechanism in the medium access control (MAC) layer according to the characteristics of mmWave flyMesh. The proposed self-healing mechanism can adaptively find an alternative link that bypasses the unusable UAV with malfunction, and the signaling overhead of self-healing can be controlled accordingly.
3) We design an efficient UAV group leader re-selection algorithm, which reduces the overhead of UAV group leader re-selection by limiting the region (number) of candidate UAV group leaders.

The remainder of this paper is organized as follows. In Section II, we describe the system model of the mmWave flyMesh. Section III presents our proposed fast beam tracking and self-healing mechanisms for the mmWave flyMesh. Efficient UAV group leader re-selection mechanism for the mmWave flyMesh is proposed in Section IV. Performance evaluation and simulation studies are carried out in Section V. Finally, Section VI concludes the paper.

II. System Model

A. The mmWave flyMesh Architecture

As shown in Fig. 1, assume each UAV is equipped with multiple antenna arrays and supports multiple beams. Each UAV can establish directional communication links with its neighboring UAVs, and thereby the mmWave flyMesh is formed. In order to provide ultra-high-speed wireless backhaul between the mmWave flyMesh and rBS, a UAV group leader

(e.g., UAV j) should be selected as the gateway based on the SINR. The remaining UAVs transmit their data to the UAV group leader, and then the UAV group leader relays the data to the rBS through the directional link between the UAV group leader and the rBS (the data of satellite is received by ground station and then ground station transmits the data to the Control Center).

Considering the practical scenarios (such as disaster rescue) of flyMesh described in Section I, there will be few rBSs. Thus, for the simplicity of analysis, the following two options are not considered in current study: 1) UAVs are not transmitting their data to the UAV group leader and just transmit their data directly to rBS; 2) there are more than one rBS. In addition, recent research on the cognitive capability harvesting network architecture [18] can also be applied to our proposed flyMesh via cognitive radio network technologies [19]. Once the UAVs are equipped with cognitive radio (CR) routers, they can harvest communication resources, such as idle spectrum bands from different locations and communication systems. Furthermore, with CR routers, UAVs are able to communicate with different devices via various interfaces, such as WiFi, cellular, Bluetooth, and Zigbee interfaces, and so on. This is important for data collection of Internet of Things (IoT) and smart cities [18]. The applications of cognitive capability harvesting network architecture will be left as our future research.

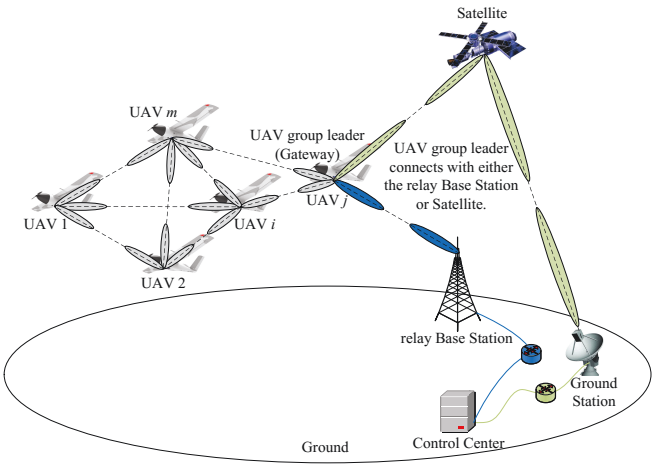

Fig. 1. The mmWave flyMesh architecture.

Assume there are m UAVs in the mmWave flyMesh and the set of UAVs is denoted as $\mathbb{M}$ = {UAV 1, UAV 2, $\cdots$, UAV m}. Further, we suppose that each UAV can generate n beams. For UAV i ($i \in [1, m]$), the set of the n beams it can generate is denoted as $\mathbb{N}_i = \{\text{beam}_1^i, \text{beam}_2^i, \cdots, \text{beam}_n^i\}$. Similarly, we assume that rBS can generate s beams and the set of the s beams is denoted as $\mathbb{S} = \{\text{beam}_1^{S/BS}, \text{beam}_2^{S/BS}, \cdots, \text{beam}_s^{S/BS}\}$. For current study, we suppose that rBS only uses one beam to establish directional communication link with the UAV group leader.

B. Beamforming Gain and Beam Pattern Model

Considering the communication links in the air are almost impossible to be multipath, we assume the links are LOS [2], [6]. We also suppose that the transmit and receive beam pairs between UAVs and between the UAV group leader and rBS are reciprocal [20]. We use the ideal antenna pattern model in [15], [21] to model the beams UAVs and rBS form. Then, the normalized beamforming gain G can be expressed as

$$G(\alpha, \vartheta) = \begin{cases} \frac{2\pi-(2\pi-\alpha)\epsilon}{\alpha}, & if\ |\vartheta| \leq \frac{\alpha}{2}, \\ \epsilon, & otherwise, \end{cases} \quad (1)$$

where α is the beamwidth of the mainlobe in radian; ϑ is the beam offset angle in radian; ϵ is the sidelobe gain and $0 < \epsilon \ll 1$.

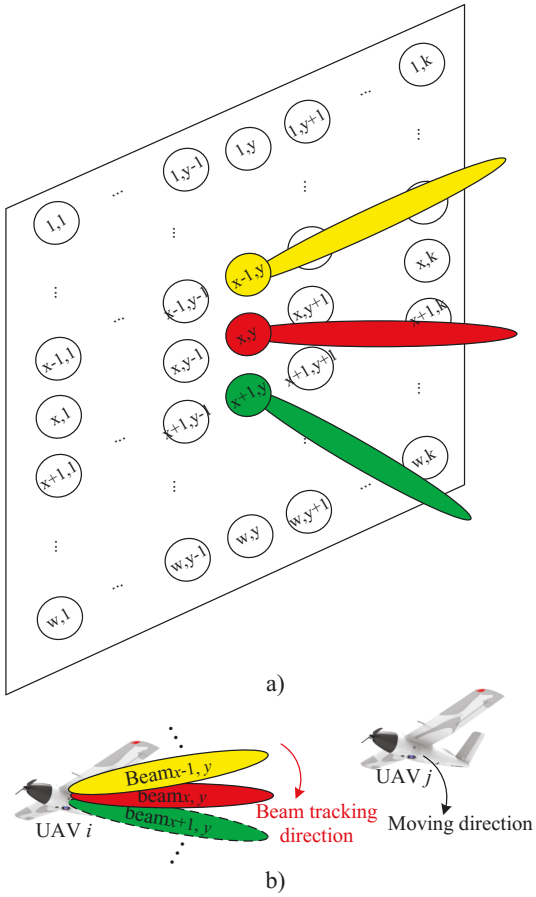

Fig. 2. Switch-based beam pattern model. a) The beam pattern of transceivers. b) An example of beam tracking (switching).

We can see from Fig. 1 that, the UAVs in the flyMesh may fly at different altitudes and the UAV group leader has to communicate with the rBS on the ground or the satellite in the air. Therefore, the mmWave antennas on the UAVs shoud cover both the horizontal and vertical dimensions. As shown in Fig. 2 a), we adopt the switch-based analog beam pattern in both transmitter and receiver [12], [13], [15], [17] by using uniform planar array (UPA) based mmWave antenna with multiple Radio Frequency (RF) chains. Because they can cover both the horizontal and vertical dimensions. With multiple RF chains, multiple beams can be generated simultaneously.

Each beam is assigned a beam identifier (i.e., $\text{beam}_{x,y}$) and covers a certain direction in a non-overlapping way. In order to cover all the directions, two UPA based mmWave antennas should be placed on the top side and the bottom side of UAVs, respectively. For each UPA of a UAV, the number of beams for each row is set to *k* and the number of beams for each column is set to *w*. Thus, for a UAV equiped with two UPAs on the top side and the bottom side, we can obtain $2k \times w = n$ based on Section II.A. For each UPA of rBS, the number of beams for each row is set to $k^{'}$ and the number of beams for each column is set to $w^{'}$. Similarly, we can get $2k^{'} \times w^{'} = s$. We can see from Fig. 2 b) that, if UAV *j* flies to the region of $\text{beam}^i_{x,y}$ from the region of $\text{beam}^i_{x-1,y}$, UAV *i* will switch to $\text{beam}^i_{x,y}$ to serve UAV *j*.

C. Channel Model and Beam Alignment

According to Friis transmission formula, the received power from a transmitter in the free space [9], [14], [15] can be determined by

$$P_r(d) = P_t \cdot G_t \cdot G_r \cdot \left(\frac{\lambda}{4\pi}\right)^2 d^{-\rho}, \tag{2}$$

where *d* is the distance between the transmitter and receiver, P_t is the transmit power, G_t is the transmit antenna gain, G_r is the receive antenna gain, λ is the wavelength, and ρ is the path loss exponent.

In Fig. 1, UAV *i* connects with UAV 1, UAV 2, UAV *m* and UAV *j*, then the received power of UAV *i* from UAV *j* can be expressed as

$$P^i_{r,j} = P^j_t \cdot G^j_{t,i}\left(\alpha^j_t, \vartheta^j_{t,i}\right) \cdot G^i_{r,j}\left(\alpha^i_r, \vartheta^i_{r,j}\right) \cdot \left(\frac{\lambda}{4\pi}\right)^2 \cdot \left(d^i_j\right)^{-\rho}, \tag{3}$$

where P^j_t is the transmit power of UAV *j*, $G^j_{t,i}\left(\alpha^j_t, \vartheta^j_{t,i}\right)$ is the transmit antenna gain of UAV *j*, $G^i_{r,j}\left(\alpha^i_r, \vartheta^i_{r,j}\right)$ is the receive antenna gain of UAV *i*, α^j_t and α^i_r are the transmit beamwidth of UAV *j* and the receive beamwidth of UAV *i*, respectively. $\vartheta^j_{t,i}$ and $\vartheta^i_{r,j}$ are the beam offset angles from the UAV *j*'s transmit beam direction to the position of UAV *i* and from the UAV *i*'s receive beam direction to the position of UAV *j*, respectively. d^i_j is the distance between UAV *j* and UAV *i*.

For the communication between UAV *i* and UAV *j*, considering the worst case that the interferences are not blocked by UAVs. Then, the interferences at UAV *i* equal to the accumulative interferences from $\mathbb{M}$ (except UAV *i* and UAV *j*). Therefore, based on (3), we can obtain the interferences at UAV *i* as in (4), where *BW* and N_0 stand for the bandwidth and the noise spectral density, respectively. In order to simplify the calculation, we neglect the interference from rBS when calculating the interferences received by UAVs. Thus, the SINR of the link between UAV *i* and UAV *j* can be expressed as in (5). Similarly, we can express the SINR of the link between UAV *j* and rBS as in (6).

Since the 802.11ay based mmWave flyMesh adopts orthogonal frequency division multiplexing (OFDM) technology, we need to consider the Doppler effect caused by the relative movement between UAVs and between the UAV group leader and rBS. From [22], we can obtain the SINR in high mobility scenarios as

$$SINR = \frac{P_s}{P_{ICI} + P_N}, \tag{7}$$

where the channel gain is normalized to one, $P_s{=}P \cdot \text{sinc}^2(f_d T_s)$ is the power of the useful signal, P_N is the power of the noise, P_{ICI} is the inter-carrier interference (ICI) power caused by the Doppler shift and it can be expressed as

$$P_{ICI} = P \cdot \left(1 - \text{sinc}^2(f_d T_s)\right), \tag{8}$$

where *P* is the transmit signal power, T_s is the OFDM symbol duration, f_d is the Doppler shift, which can be expressed as

$$f_d = \frac{f_c \cdot v}{c} \cdot \cos\varphi, \tag{9}$$

where f_c is the carrier frequency, *v* is the relative moving speed, $c{=}3{\times}10^8$ m/s, and φ is the angle between the receiving direction of the receiver and the moving direction of the transmitter.

Therefore, after considering the Doppler shift, the SINR values between UAV *i* and UAV *j* and between UAV *j* and rBS can be rewritten as in (10) and (11), respectively. Here, $f^{j,i}_d$ and $f^{S/BS,j}_d$ stand for the Doppler shift between UAV *i* and UAV *j* and between UAV *j* and rBS, respectively. $f^{e,i}_d$ and $f^{e,j}_d$ stand for the Doppler shift between UAV *i* and UAV *e* and between UAV *j* and UAV *e*, respectively.

Assume there are a large number of UAVs and each UAV can find its neighboring UAVs to establish directional communication links. Then, we can get the requirement of the beam alignment between UAV *i* and UAV *j* from [23], and the best beam pair can be obtained by solving the following optimization problem:

$$\{\text{beam}^i_{x*,y*}, \text{beam}^j_{x^{'}*,y^{'}*}\} = \underset{\substack{x=1,\cdots,2k;y=1,\cdots,w \\ x^{'}=1,\cdots,2k;y^{'}=1,\cdots,w}}{\arg\max} SINR^i_j. \tag{12}$$

According to (1), if two beams are aligned, then $\vartheta^j_{t,i} = \vartheta^j_{r,i} = 0$. Thus, we can get

$$G^j_{t,i}\left(\alpha^j_t, \vartheta^j_{t,i}\right) = \frac{2\pi - (2\pi - \alpha^j_t)\epsilon}{\alpha^j_t}, |\vartheta^j_{t,i}| \le \frac{\alpha^j_t}{2}, \tag{13a}$$

$$G^i_{r,j}\left(\alpha^i_r, \vartheta^i_{r,j}\right) = \frac{2\pi - (2\pi - \alpha^i_r)\epsilon}{\alpha^i_r}, |\vartheta^i_{r,j}| \le \frac{\alpha^i_r}{2}. \tag{13b}$$

Similarly, we can obtain the best beam pair between UAV *j* and rBS by solving the following optimization problem:

$$\{\text{beam}^j_{x*,y*}, \text{beam}^{S/BS}_{x^{'}*,y^{'}*}\} = \underset{\substack{x=1,\cdots,2k;y=1,\cdots,w \\ x^{'}=1,\cdots,2k^{'};y^{'}=1,\cdots,w^{'}}}{\arg\max} SINR^j_{S/BS}. \tag{14}$$

III. Beam Management and Self-healing

Although the flyMesh can be flexibly formed and the network connectivity can be adjusted at any time to accommodate the change of relative position between UAVs, there are still many challenges in the mmWave based flyMesh. The relative movement between UAVs or between the UAV group leader and rBS will make the directional transmissions very unstable, which requires frequent beam tracking or other beam realignment operations (e.g., beam training). However, the beam

$$P_{I,i} = \sum_{e\in\{S/BS\bigcup \mathbb{M}\setminus(i,j)\}} P_t^e \cdot G_{t,i}^e\left(\alpha_t^e, \vartheta_{t,i}^e\right) \cdot G_{r,e}^i\left(\alpha_r^i, \vartheta_{r,e}^i\right) \cdot \left(\frac{\lambda}{4\pi}\right)^2 \cdot \left(d_e^i\right)^{-\rho} + BW \cdot N_0. \tag{4}$$

$$SINR_j^i = \frac{P_t^j \cdot G_{t,i}^j\left(\alpha_t^j, \vartheta_{t,i}^j\right) \cdot G_{r,j}^i\left(\alpha_r^i, \vartheta_{r,j}^i\right) \cdot \left(\frac{\lambda}{4\pi}\right)^2 \cdot \left(d_j^i\right)^{-\rho}}{\sum\limits_{e\in\{S/BS\bigcup \mathbb{M}\setminus(i,j)\}} P_t^e \cdot G_{t,i}^e\left(\alpha_t^e, \vartheta_{t,i}^e\right) \cdot G_{r,e}^i\left(\alpha_r^i, \vartheta_{r,e}^i\right) \cdot \left(\frac{\lambda}{4\pi}\right)^2 \cdot \left(d_e^i\right)^{-\rho} + BW \cdot N_0}. \tag{5}$$

$$SINR_{S/BS}^j = \frac{P_t^{S/BS} \cdot G_{t,j}^{S/BS}\left(\alpha_t^{S/BS}, \vartheta_{t,j}^{S/BS}\right) \cdot G_{r,S/BS}^j\left(\alpha_r^j, \vartheta_{r,S/BS}^j\right) \cdot \left(\frac{\lambda}{4\pi}\right)^2 \cdot \left(d_{S/BS}^j\right)^{-\rho}}{\sum\limits_{e\in\mathbb{M}\setminus j} P_t^e \cdot G_{t,j}^e\left(\alpha_t^e, \vartheta_{t,j}^e\right) \cdot G_{r,e}^j\left(\alpha_r^j, \vartheta_{r,e}^j\right) \cdot \left(\frac{\lambda}{4\pi}\right)^2 \cdot \left(d_e^j\right)^{-\rho} + BW \cdot N_0}. \tag{6}$$

$$SINR_j^i = \frac{P_t^j \cdot \mathrm{sinc}^2(f_d^{j,i}T_s) \cdot G_{t,i}^j\left(\alpha_t^j, \vartheta_{t,i}^j\right) \cdot G_{r,j}^i\left(\alpha_r^i, \vartheta_{r,j}^i\right) \cdot \left(\frac{\lambda}{4\pi}\right)^2 \cdot \left(d_j^i\right)^{-\rho}}{\underbrace{\sum\limits_{e\in\{S/BS\bigcup \mathbb{M}\setminus(i,j)\}} P_t^e \cdot G_{t,i}^e\left(\alpha_t^e, \vartheta_{t,i}^e\right) \cdot G_{r,e}^i\left(\alpha_r^i, \vartheta_{r,e}^i\right) \cdot \left(\frac{\lambda}{4\pi}\right)^2 \cdot \left(d_e^i\right)^{-\rho}}_{\text{interference from other UAVs}} + \underbrace{BW \cdot N_0}_{\text{noise}} + \underbrace{P_t^j \cdot \left(1 - \mathrm{sinc}^2(f_d^{j,i}T_s)\right) \cdot G_{t,i}^j\left(\alpha_t^j, \vartheta_{t,i}^j\right) \cdot G_{r,j}^i\left(\alpha_r^i, \vartheta_{r,j}^i\right) \cdot \left(\frac{\lambda}{4\pi}\right)^2 \cdot \left(d_j^i\right)^{-\rho}}_{\text{interference from ICI of UAV}j}}, \tag{10}$$

$$SINR_{S/BS}^j = \frac{P_t^{S/BS} \cdot \mathrm{sinc}^2(f_d^{S/BS,j}T_s) \cdot G_{t,j}^{S/BS}\left(\alpha_t^{S/BS}, \vartheta_{t,j}^{S/BS}\right) \cdot G_{r,S/BS}^j\left(\alpha_r^j, \vartheta_{r,S/BS}^j\right) \cdot \left(\frac{\lambda}{4\pi}\right)^2 \cdot \left(d_{S/BS}^j\right)^{-\rho}}{\underbrace{\sum\limits_{e\in\mathbb{M}\setminus j} P_t^e \cdot G_{t,j}^e\left(\alpha_t^e, \vartheta_{t,j}^e\right) \cdot G_{r,e}^j\left(\alpha_r^j, \vartheta_{r,e}^j\right) \cdot \left(\frac{\lambda}{4\pi}\right)^2 \cdot \left(d_e^j\right)^{-\rho}}_{\text{interference from other UAVs}} + \underbrace{BW \cdot N_0}_{\text{noise}} + \underbrace{P_t^{S/BS} \cdot \left(1 - \mathrm{sinc}^2(f_d^{S/BS,j}T_s)\right) \cdot G_{t,j}^{S/BS}\left(\alpha_t^{S/BS}, \vartheta_{t,j}^{S/BS}\right) \cdot G_{r,S/BS}^j\left(\alpha_r^j, \vartheta_{r,S/BS}^j\right) \cdot \left(\frac{\lambda}{4\pi}\right)^2 \cdot \left(d_{S/BS}^j\right)^{-\rho}}_{\text{interference from ICI of S/BS}}}, \tag{11}$$

training mechanism based on traditional exhaustive search is too time-consuming [12], [13], [17], and it is a waste of communication opportunities for battery powered UAVs [1], [6]. Therefore, efficient and accurate beam tracking mechanisms are needed to reduce the beam alignment overhead/time.

A. Fast Beam Tracking for mmWave flyMesh

In this study, we propose a fast beam tracking mechanism, which is based on the beam tracking mechanism of 802.11ad/ay. Fig. 3 shows the beam tracking mechanism of 802.11ad/ay, if the link quality (i.e., SINR) falls below the threshold η_1, we can infer that this link is not good enough for communications (although this link is not actually disconnected, and it can also be used for data transmission at a low data rate) [12], [13]. An alternative link with higher quality (larger than η_1) should be found to complete the subsequent data transmissions. Thus, the beam tracking initiator can append TRN-T (Transmit Training) units to the next Data frame to perform transmit beam tracking. TRN-T units are the training sequences that can be used to train multiple different transmit beams [12], [13], [17]. Next, the beam tracking responder will feed back the beam tracking results to the beam tracking initiator by appending a beam refinement protocol (BRP) frame to the end of the Ack frame. According to the results brought by the BRP frame, the beam tracking initiator selects the best beam as the new transmit beam for the subsequent data transmissions. Similarly, if receive beam tracking is needed, TRN-R (Receive Training) units can be appended to the Data frame to perform receive beam tracking. For more details, readers are referred to [12], [13], [17].

In order to solve the optimization problem (12), all the beams should be searched to find the best beam pair. However, it is time-consuming and complicated for the battery powered UAVs. Thus, we propose a fast beam tracking mechanism to find the suboptimal solution of (12) in mobile scenarios based on the beam tracking mechanism in [12], [13] and the switch-based beam pattern model in Section II.B. Initially, we assume UAV *i* communicates with UAV *j* through beam pair $\{\mathrm{beam}_{x,y}^i, \mathrm{beam}_{x',y'}^j\}$. If $SINR_j^i < \eta_1$, UAV *i* indicates "Fast Beam Tracking Requested" in the next Data frame to start fast beam tracking and selects a beam set $\mathbf{N}_i^{test1}$ = { $\mathrm{beam}_{x-1,y-1}^i$, $\mathrm{beam}_{x-1,y}^i$, $\mathrm{beam}_{x-1,y+1}^i$, $\mathrm{beam}_{x,y-1}^i$, $\mathrm{beam}_{x,y+1}^i$, $\mathrm{beam}_{x+1,y-1}^i$, $\mathrm{beam}_{x+1,y}^i$, $\mathrm{beam}_{x+1,y+1}^i$ } around $\mathrm{beam}_{x,y}^i$ to append to the TRN-T units. Then, UAV *j* feeds back the results of beam tracking to UAV *i*. If all the SINR values are less than $SINR_j^i$, which implies

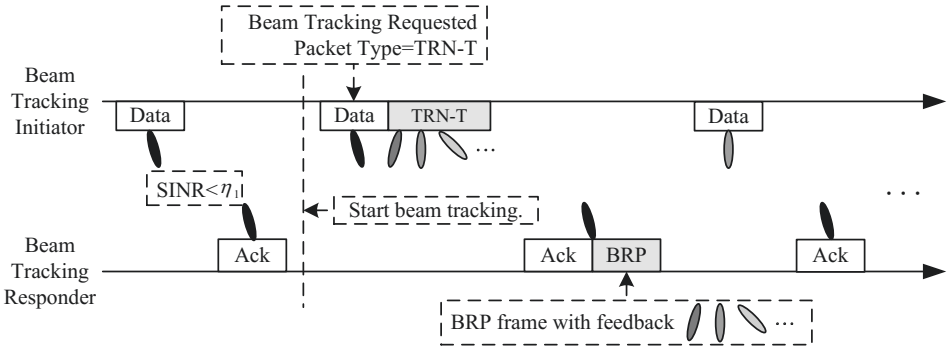

Fig. 3. An example of beam tracking with TRN-T units appended.

that UAV *i* and UAV *j* is flying away from each other, then it is impossible for UAV *i* and UAV *j* to recover the link $\mathrm{beam}^i_{x,y} \rightarrow \mathrm{beam}^j_{x',y'}$. They should re-establish communication links with other neighboring UAVs. If the SINR value(s) is (are) greater than $SINR^i_j$, UAV *i* should select the beam with the maximum SINR (e.g., $\mathrm{beam}^i_{x,y+1}$) as the new transmit beam to continue the next beam tracking operation. Then, UAV *i* selects another beam set $\mathbf{N}^{test2}_i = \{\mathrm{beam}^i_{x-1,y+2}, \mathrm{beam}^i_{x,y+2}, \mathrm{beam}^i_{x+1,y+2}\}$ around $\mathrm{beam}^i_{x,y+1}$ to append to the TRN-T units. Similarly, for the subsequent beam operations, UAV *i* will select the beams around the beam with maximum SINR in the current beam tracking to update $\mathbf{N}^{test2}_i$. Furthermore, we set another threshold η_2. Once the SINR value(s) of the beam tracking results is (are) higher than or equal to η_2, beam tracking can be stopped and the corresponding link quality can be considered as good enough for high speed data transmission [14], [24]. The detailed fast beam tracking algorithm is summarized in Algorithm 1.

The relative movement between UAVs and between the UAV group leader and rBS may be continuous. The proposed fast beam tracking can infer the relative moving direction through the variations of SINR values obtained by beam tracking. Thus, fast beam tracking can flexibly adjust the next beam tracking region (i.e., $\mathbf{N}^{test2}_i$) through self-learning based on the current beam tracking results. However, the traditional beam tracking algorithm proposed in 802.11ad/ay standard cannot do that. This is the difference between our proposed algorithm and the beam tracking algorithm used in 802.11ad/ay. Therefore, to achieve beam alignment, the number of candidate beams that need to be tracked can be reduced. Similarly, Algorithm 1 is also applicable to the beam tracking between the UAV group leader and rBS. In addition, we use fixed wing UAVs in this paper. Therefore, there is almost no chance for UAVs have a tendency to rotate on their own axis. Even for the rotor UAVs may have a tendency to rotate on their own axis which would cause beam misalignment when they are not really moving at very high speeds, the proposed fast beam tracking can also solve this problem. However, due to the page, we will not repeat how the proposed fast beam tracking is applied to the two scenarios mentioned above.

We use the beam pattern model introduced in Section II.B to analyze the performance of fast beam tracking. The number

Algorithm 1 Fast Beam Tracking Algorithm.

1: UAV *i* communicates with UAV *j* through beam pair $\{\mathrm{beam}^i_{x,y}, \mathrm{beam}^j_{x',y'}\}$;
2: **if** $SINR^i_j < \eta_1$ **then**
3: UAV *i* appends $\mathbf{N}^{test1}_i$ to the TRN-T units;
4: UAV *j* feeds back the SINR values of the corresponding beam pairs $\{\mathrm{beam}^i_{\substack{x=x-1,x,x+1\\y=y-1,y,y+1}}, \mathrm{beam}^j_{x',y'}\}$;
5: **if** all the SINR values of $\{\mathrm{beam}^i_{\substack{x=x-1,x,x+1\\y=y-1,y,y+1}}, \mathrm{beam}^j_{x',y'}\} < SINR^i_j$ **then**
6: quit the beam tracking, and redo the beamforming training with their neighboring UAVs;
7: **else if** the SINR value(s) of $\{\mathrm{beam}^i_{\substack{x=x-1,x,x+1\\y=y-1,y,y+1}}, \mathrm{beam}^j_{x',y'}\} \geq \eta_2$ **then**
8: UAV *i* selects the beam pair $\{\mathrm{beam}^i_{x_*,y_*}, \mathrm{beam}^j_{x',y'}\}$ with the maximum SINR value transmits the subsequent Data frames through $\mathrm{beam}^i_{x_*,y_*}$, quit the beam tracking;
9: **else if** the SINR value(s) of $\{\mathrm{beam}^i_{\substack{x=x-1,x,x+1\\y=y-1,y,y+1}}, \mathrm{beam}^j_{x',y'}\} \geq \eta_1$, but all the SINR values of $\{\mathrm{beam}^i_{\substack{x=x-1,x,x+1\\y=y-1,y,y+1}}, \mathrm{beam}^j_{x',y'}\} < \eta_2$ **then**
10: UAV *i* selects the beam pair $\{\mathrm{beam}^i_{x_*,y_*}, \mathrm{beam}^j_{x',y'}\}$ with the maximum SINR value, appends $\mathbf{N}^{test2}_i$ to the TRN-T units and goes to step 4;
11: **end if**
12: **else**
13: UAV *i* continues to communicate with UAV *j* through beam pair $\{\mathrm{beam}^i_{x,y}, \mathrm{beam}^j_{x',y'}\}$;
14: **end if**

of beams in $\mathbf{N}^{test1}_i$ is set to N_{test1}, and the number of beams in $\mathbf{N}^{test2}_i$ is set to N_{test2}. Taking transmit (or receive) beam tracking as an example, each beam direction corresponds to a TRN(-T) unit when the beam tracking is performed. In order to achieve the result in (12), we can obtain the overhead of the fast beam tracking (i.e., the number of TRN units required) with a given beam offset angle (ϑ) and the beamwidth (α) as

$$N_{Fast,TRN} = N_{test1} + \left(\frac{\vartheta}{\alpha} - 1\right) \cdot N_{test2}. \tag{15}$$

However, the overhead of the beam tracking in 802.11ad/ay

can be expressed as

$$N_{802.11\text{ay},TRN} = \left(2 \cdot \frac{\vartheta}{\alpha} + 1\right)^2 - 1. \quad (16)$$

Proof: The proof is provided in Appendix A. ■

B. Self-healing for the mmWave flyMesh

In order to ensure the robustness of the mmWave flyMesh, just adopting the fast beam tracking mechanism is not enough to meet the demand. Because the mmWave flyMesh is easily affected by environmental conditions or its own power constraint in practical applications, which makes some UAVs malfunctioning or unusable and thus affects the full connectivity of the mmWave flyMesh. Actually, the probability of UAVs becoming malfunctioning or unusable is hard to be modeled in practical applications. Therefore, we do not focus on the reasons and the probability that UAVs become unusable. We focus on how to realize the instant and quick self-healing of the mmWave flyMesh once the UAVs become unusable. For analytical tractability, we simplify the mmWave flyMesh as a planar graph just like, for example, the two-dimensional (2D) flyMesh as shown in Fig. 4.

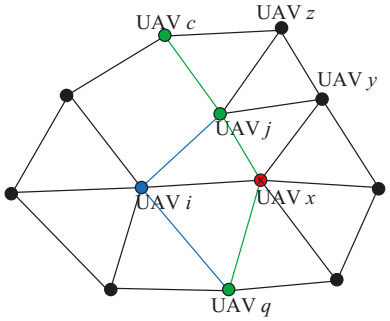

Fig. 4. Two-dimensional mmWave flyMesh graph.

Suppose UAV c acts as the UAV group leader and connects with rBS (please refer to Fig. 1), and it has data to transmit to UAV q. For a certain link UAV c → UAV j → UAV x → UAV q, if UAV x becomes unusable, it is too far to establish a high quality link between UAV j and UAV q through beam management (e.g., beam training or beam tracking). At this point, another link (e.g., UAV c → UAV j → UAV i → UAV q) should be found from the network layer to replace the weak link. However, it poses a significant challenge for the flyMesh to find an appropriate link to replace the weak link from the network layer [25]. Therefore, we propose a self-healing mechanism from the MAC layer to achieve local link recovery when the MAC layer transmission failure occurs [26], [27]. An instant and quick forwarding link can be found and just bypasses the unusable UAV before the routing timer of the network layer reaches zero. Thereby, it will form an illusion of sustainable link in the network layer, and the self-healing will be transparent to the network layer. However, when significant change of the network topology occurs or a majority of UAVs become unusable, re-routing is also needed from the network layer, which will be addressed elsewhere.

1) Frame structure and signaling design: When a UAV becomes unusable, in order to ensure that the upstream UAV of the unusable UAV can find an alternative forwarding link through the MAC layer, we should design new frames and signalings first. The Self-healing Request and Self-healing Response frames are defined for finding forwarding links based on [12], [13] as shown in Fig 5, where

- RA is the address of the receiver;
- TA is the address of the transmitter;
- DA is the address of the destination UAV;
- SA is the address of the source UAV;
- NA is the address of the unusable UAV;
- "Nearby = DA?" = 1 indicates that this UAV is directly connected to the destination UAV, otherwise it is not directly connected to the destination UAV;
- "Nearby = NA?" = 1 represents this UAV is directly connected to the unusable UAV, otherwise it is not directly connected to the unusable UAV.

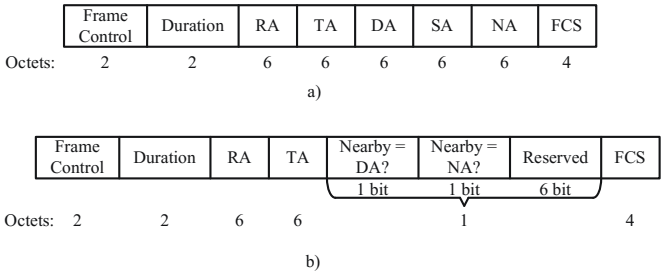

Fig. 5. a) Self-healing Request frame format. b) Self-healing Response frame format.

2) Self-healing mechanism: As shown in Fig. 4, we assume that there is only one UAV that becomes unusable. If we redefine the Self-healing Request frame by adding multiple NA fields, this self-healing mechanism can be applied to the condition that multiple UAVs become unusable as well. Taking UAV c → UAV j → UAV x → UAV q as an example, if UAV j transmits Data frame to UAV x, and UAV j cannot receive Ack frame from UAV x, UAV j will re-transmit this Data frame to UAV x. We define a maximum re-transmission limit N_{retry}. If UAV j re-transmits for N_{retry} times and it still cannot receive Ack frame from UAV x, UAV j will consider UAV x unusable. Since the flyMesh is a mesh network, a UAV will connect with its neighboring UAVs by directional beams. Thus, the neighboring UAVs can receive packets from UAV j at any time. Then, UAV j will transmit Self-healing Request frames to the UAVs who are directly connected with it (e.g., UAV i, UAV y and UAV z). At this point, the RAs of the transmitted Self-healing frames are UAV i, UAV y and UAV z, respectively; the TAs are UAV j; the DAs are UAV q; the SAs are UAV c and the NAs are UAV x. The UAV receiving the Self-healing Request frame will compare the DA and NA with its neighboring UAVs and then feed back a Self-healing Response frame to UAV j. Thus, the following operations are carried out as follows:

- If all the UAVs that receive the Self-healing Request frame find that their neighboring UAVs are not indicated

in the DA and NA fields, these UAVs will feed back the Self-Response frames with "Nearby=DA?" = 0 and "Nearby=NA?" = 0. After UAV *j* receiving the Self-Response frames, it will permit these UAVs to continue the next self-healing operation;

- If a UAV receives the Self-healing Request frame and finds that one of its neighboring UAVs is indicated in the NA field, but there is no neighboring UAVs indicated in the DA field. This UAV will feed back the Self-Response frame with "Nearby=DA?" = 0 and "Nearby=NA?" = 1. After UAV *j* receiving the Self-Response frame, it will permit this UAV to continue the next self-healing operation and forbid other UAVs to continue the next self-healing operations;
- If a UAV receives the Self-healing Request frame and finds that one of its neighboring UAV is indicated in the DA field, which means the destination UAV is found. This UAV will feed back the Self-Response frames with "Nearby=DA?" = 1. After UAV *j* receiving the Self-Response frame, UAV *j* declares to quit self-healing operation.

The proposed self-healing mechanism can spread out to find the suitable UAVs if there is no neighboring UAV indicated in the NA field. Once the UAV whose neighboring UAV is indicated in the DA or NA field is found, the searching area will be limited just around this UAV and the other UAVs will stop searching again. Since the searching area is limited to the surrounding of the unusable UAV, an instant and quick forwarding link just bypassing the unusable UAV can be established. Although the proposed self-healing mechanism may not find the optimal forwarding link and may not be the optimal solution to recovering the mmWave flyMesh, we aim to find an instant and quick forwarding link to achieve the self-healing of the mmWave flyMesh with small signaling overhead. The proposed self-healing mechanism can be summarized as in Algorithm 2. It is worth noting that the unusable UAV should be one of the intermediate nodes of the flyMesh in the proposed self-healing mechanism. If the source UAV is suddenly not working, there is no upstream UAV of the source UAV, thus self-healing will not be carried out.

According to Section II.A, we know that there are *m* UAVs in the mmWave flyMesh. Assuming there are m_{out} UAVs on the boundary of the mmWave flyMesh and the remaining m_{in} (where $m_{in} = m - m_{out}$) UAVs is internal UAVs of the mmWave flyMesh (e.g., UAV *i*, UAV *j* and UAV *x* in Fig. 4). For the m_{in} internal UAVs of the mmWave flyMesh, suppose each UAV connects with $n_{in,near}$ neighboring UAVs. For the m_{out} UAVs on the boundary of the mmWave flyMesh, suppose each UAV connects with $n_{out,near}$ neighboring UAVs. We use a MAC protocol modified based on Ad hoc On-demand Distance Vector Routing (AODV) protocol [30] as a comparison of the proposed self-healing mechanism (noticing that there is no related network self-healing method in the MAC layer in the original AODV). In addition, the MAC layer has no routing table, it is impractical to fully transplant AODV to the MAC layer. In the MAC protocol modified based on AODV, the source UAV broadcasts request signaling

Algorithm 2 Self-healing Algorithm.

```
UAV j transmits Data_i to UAV x;
if UAV j receives Ack from UAV x then
    UAV j continues transmitting the rest Data frames to UAV x;
else
    UAV j re-transmits Data_i to UAV x;
    if re-transmission times ≤ N_retry and UAV j receives Ack from UAV x then
        UAV j continues transmitting the rest Data frames to UAV x;
    else if re-transmission times > N_retry then
        UAV j transmits the Self-healing Request frames to the UAVs around itself;
        The UAVs received the Self-healing Request frame feeds back Self-healing Response frames to UAV j;
        if "Nearby=DA?"=0&&"Nearby=NA?"=0 then
            UAV j allows the UAVs around it to continue to transmit the Self-healing Request frames, go to step 10;
        else if "Nearby=DA?"=0&&"Nearby=NA?"=1 then
            UAV j allows the UAV who feeds back "Nearby = NA?" = 1 to continue to transmit the Self-healing Request frame and forbids the other UAVs to transmit the Self-healing Request frames, go to step 10;
        else if "Nearby=DA?"=1 then
            the destination UAV is found; quit self-healing operation;
        end if
    end if
end if
```

to its neighboring UAVs, if there is no destination UAV, the source UAV's neighboring UAVs will broadcast request signaling again to their neighboring UAVs, respectively, until the destination UAV is found. However, there is a limitation that the links should not be requested twice. For example, if UAV *c* transmit a request signaling to UAV *j*, UAV *j* will not transmit request signaling to UAV *c* again. Thus, the signaling overhead (i.e., the total number of searching times) for finding the forwarding link is

$$O_{tra} \approx \frac{m_{in} \cdot n_{in.near} + m_{out} \cdot n_{out.near}}{2}. \tag{17}$$

However, if the proposed self-healing mechanism is performed, and assume the upstream UAV (e.g., UAV *j* in Fig. 4) of the unusable UAV (e.g., UAV *x* in Fig. 4) needs S_{self} steps to find the downstream UAV (e.g., UAV q in Fig. 4) of the unusable UAV, the signaling overhead (i.e., the total number of searching times) can be expressed as

$$O_{self} \leq (n_{in,near} - 1)^{s_{self}} - 1. \tag{18}$$

Proof: The proof is provided in Appendix B. ■

IV. Efficient UAV Group Leader Re-Selection

UAV group leader is crucial to the mmWave flyMesh, since it will collect all UAVs' data and transmit it to rBS. The link between the UAV group leader and rBS requires ultra-high-speed wireless transmissions [1]. However, due to the mobility of the mmWave flyMesh, the beam alignment between the UAV group leader and rBS should be performed to ensure high link quality. Although the fast beam tracking mechanism proposed in Section III.A is flexible enough to achieve the beam alignment, it cannot cope with the link interruption caused by the UAV group leader flying far away from rBS.

In this situation, it is necessary to select another UAV as an alternative UAV group leader to provide ultra-high-speed wireless backhaul.

For the simplicity of analysis, we simplify the topology in Fig. 1 into the 2D flyMesh as shown in Fig. 6. Assume UAV *j* has established the directional communication link with rBS with beam pair $\{\text{beam}_{x,y}^{j}, \text{beam}_{x',y'}^{S/BS}\}$. Through the analysis of Section II.C, we can get the condition on which alternative UAV group leader to replace UAV *j*: the SINR between UAV *j* and rBS drops below η_1, and all the SINR values obtained from the beam tracking in $\mathbf{N}_j^{test1}$ are lower than $SINR_{S/BS}^{j}$. If there is no prior information for UAV group leader re-selection, rBS will perform beam training with all UAVs around itself to find an optimal UAV group leader. Too many inappropriate UAVs (e.g., the UAVs flying away from rBS) performing beam training with rBS will result in very high overhead due to the UAV group leader re-selection, which will cause long delay for the backhaul link. Therefore, we propose an efficient UAV group leader re-selection mechanism to solve this problem.

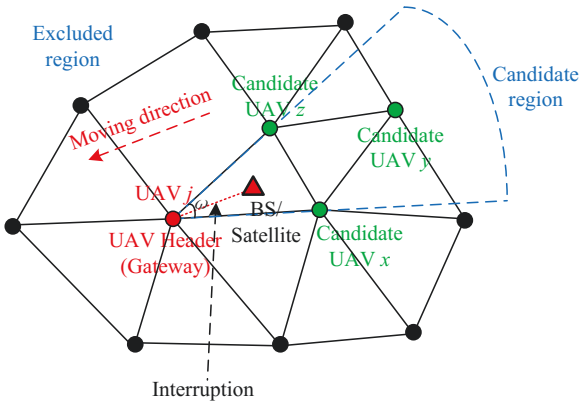

Fig. 6. UAV group leader re-selection diagram for mmWave flyMesh.

As shown in Fig. 6, in order to lower the overhead due to UAV group leader re-selection, the number of candidate UAV group leader should be reduced. For UAV *j*, it should mark $\text{beam}_{x,y}^{j}$ as the starting point and search for the first UAV around it from two directions, clockwise and counterclockwise, respectively (e.g., UAV *z* is the first candidate UAV group leader searched from counterclockwise and UAV *x* is the first candidate UAV group leader searched from clockwise). We denote the angle between the link from UAV *j* to candidate UAV *z* and the link from UAV *j* to candidate UAV *x* as ω (the unit is radian), and then the region corresponding to ω can be considered as the candidate region and the other region is considered as the excluded region. Obviously, there is no need for the UAVs in the excluded region to perform beam training with rBS, thus the UAV group leader re-selection overhead can be reduced. In order to determine the other appropriate candidate UAV group leaders in the candidate region, the opposite beam direction $\text{beam}_{ox,oy}^{z}$ of $\text{beam}_{x,y}^{z}$ and the opposite beam direction $\text{beam}_{ox,oy}^{x}$ of $\text{beam}_{x,y}^{x}$ should be obtained based on the beam pattern model as shown in Fig. 2. Then, UAV *z* should search for the UAVs toward rBS's direction from $\text{beam}_{x,y}^{z}$ to $\text{beam}_{ox,oy}^{z}$ and UAV *x* should search for the UAVs toward rBS's direction from $\text{beam}_{x,y}^{x}$ to $\text{beam}_{ox,oy}^{x}$. We denote the set of UAVs searched in the candidate region as $\mathbb{M}_{candi}$, and then rBS performs beam training with the UAVs in $\mathbb{M}_{candi}$. Thus, the new UAV group leader (e.g., UAV *e*) satisfies $\max_{e\in\mathbb{M}_{candi}} SINR_{S/BS}^{e}$. That is to say, the UAV with the maximum SINR will be selected by rBS as the new UAV group leader. The proposed efficient UAV group leader re-selection mechanism can be summarized as in Algorithm 3.

Algorithm 3 Efficient UAV Group Leader Re-Selection Algorithm.

1: UAV *j* communicates with rBS through beam pair $\{\text{beam}_{x,y}^{j}, \text{beam}_{x',y'}^{S/BS}\}$;
2: **if** $SINR_{S/BS}^{j} < \eta_1$ **then**
3: UAV *j* indicates "Fast Beam Tracking Requested" in the next Data frame and appends $\mathbf{N}_j^{test1}$ to the TRN-T units;
4: rBS feeds back the SINR values of the corresponding beam pairs $\{\underset{\substack{x=x-1,x,x+1\\y=y-1,y,y+1}}{\text{beam}_{x,y}^{j}}, \text{beam}_{x',y'}^{S/BS}\}$;
5: **if** all the SINR values of $\{\underset{\substack{x=x-1,x,x+1\\y=y-1,y,y+1}}{\text{beam}_{x,y}^{j}}, \text{beam}_{x',y'}^{S/BS}\} < SINR_{S/BS}^{j}$ **then**
6: UAV *j* marks $\text{beam}_{x,y}^{j}$ as the starting point, searches for the first UAV around it from two directions, clockwise and counterclockwise, respectively;
7: The two UAVs searched in step 6 continue searching for other UAVs toward rBS's direction from $\text{beam}_{x,y}^{cand1}$ to $\text{beam}_{ox,oy}^{cand1}$ and from $\text{beam}_{x,y}^{cand2}$ to $\text{beam}_{ox,oy}^{cand2}$, respectively;
8: After searching for all the UAVs in the candidate region, rBS performs the beam training with all the candidate UAV group leaders;
9: rBS selects the UAV with the maximum SINR value based on the results of the beam training as a new UAV group leader (Gateway);
10: **end if**
11: **else**
12: UAV *j* performs fast beam tracking (Algorithm 1);
13: **end if**

According to [15], [16], the number of beam training times between UAV *j* and rBS can be expressed as

$$N_{Training}^{UAV,S/BS} = n \cdot s, \tag{19}$$

where *n* and *s* are the number of beams UAV and rBS form, respectively.

We know from [12], [13], [16] that, with the same number of beams trained for each user, the overhead of the beam training is proportional to the number of users. If Algorithm 3 is not adopted, the number of beam training times for completing the UAV group leader re-selection is

$$N_{re-selection}^{normal} = \left|\left\{e \in \mathbb{M} \mid SINR_{S/BS}^{e} > SINR_{S/BS}^{j}\right\}\right| \cdot n \cdot s, \tag{20}$$

where $|\cdot|$ denotes the cardinality of a set.

However, if Algorithm 3 is adopted, the number of candidate UAV group leaders can be reduced based on the prior information. Assuming there are m_{candi} UAVs in $\mathbb{M}_{candi}$, the

number of beam training times becomes

$$N_{re-selection}^{efficient} = m_{candi} \cdot n \cdot s \approx \frac{\omega}{2\pi} \cdot \left| \left\{ e \in \mathbb{M} \mid SNIR_{S/BS}^{e} > SNIR_{S/BS}^{j} \right\} \right| \cdot n \cdot s. \quad (21)$$

It is worth noting that, for UAV, which is not the group leader, it will only execute Algorithm 1 and Algorithm 2. If the quality of the directional link is weak (but the quality is still enough to maintain communication), then Algorithm 1 will be executed. However, if the directional link is broken, then Algorithm 2 will be executed. For UAV, which is the group leader, if the quality of the directional link is weak (but the quality is still enough to maintain communication), then Algorithm 3 will be executed.

V. Performance Evaluation

In this section, we will present the performance analysis and simulation results of the proposed fast beam tracking, self-healing and efficient UAV group leader re-selection mechanisms. The simulation parameters [4], [12], [13], [29], [30] are listed in Table I. When the path loss exponent ρ is set to 2, the path loss in (2) can be rewritten as $PL[dB] = 32.5 + 20log_{10}(f_c) + 20log_{10}(d)$. The power of noise $N_0[dBm] = -174[dBm/Hz] + 10log_{10}(BW) + NF[dB]$, where *NF* is the noise figure in dB [15]. In order to be more intuitive, the unit of the beamwidths (α) and the beam angle offsets (ϑ) are converted into degrees. For the flyMesh, all UAVs are randomly distributed and fly in the same direction. In addition, we set the radius of the flyMesh and the minimum distance between two UAVs to 500 m and 10 m, respectively. Therefore, if there are more UAVs (i.e., from 10 to 50) in the flyMesh, the distribution density of UAVs will be larger.

TABLE I
Simulation Parameters.

Parameters	Values
Carrier frequency, f_c	60 GHz
Bandwidth, BW	2.16 GHz
Subcarrier spacing, Δf	5.15625 MHz
Transmit power, P_t	20 dBm
Beamwidth, α	10°, 20°, 30°
The side lobe gain, ϵ	0.01
SINR threshold, η_1	20 dB
SINR threshold, η_2	30 dB
Noise figure, *NF*	6 dB

A. The performance of fast beam tracking mechanism

To evaluate the performance of our proposed fast beam tracking, we choose the mechanism of 802.11ay beam tracking as the comparison reference. Moreover, we have briefly described the 802.11ay beam tracking in Fig. 3 and Section III.A. As for our proposed fast beam tracking (i.e., Algorithm 1), the first beam tracking step will track the beams in $\mathbf{N}_i^{test1}$. Then, for the second beam tracking step, the beams in $\mathbf{N}_i^{test2}$ can be obtained from the results of the first beam tracking step. Next, the subsequent beam tracking steps will adopt the beams in the updated $\mathbf{N}_i^{test2}$ based on the previous beam tracking results. Assume the beamwidths (α) of the transmitter and receiver are 10°, and the beam angle offsets (ϑ) caused by relative movements are 10°, 20°, 30°, 40°, 50°, 60°, 70°, 80°, 90°, respectively. Based on the beam pattern model in Fig. 2, we set N_{test1} to 8 and N_{test2} to 3. The performance comparison between the fast beam tracking and 802.11ay beam tracking is shown in Fig. 7. We can see from Fig. 7 that, the performance of fast beam tracking is much better than that of the 802.11ay. Furthermore, with the increase of beam angle offset, the beam tracking overhead of fast beam tracking increases slowly, while the overhead of the 802.11ay beam tracking increases significantly. This is because the fast beam tracking can flexibly adjust the next beam tracking region based on the current beam tracking results. Thus, with the given beam angle offset, the proposed fast beam tracking can achieve beam alignment with low overhead, which is very important for the sustainability limited UAV wireless communications.

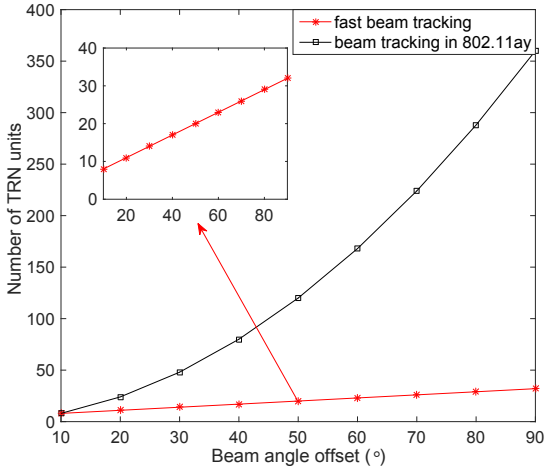

Fig. 7. The performance comparison between the fast beam tracking and 802.11ay beam tracking with different beam angle offsets.

Fig. 8 shows the performance comparison between the proposed fast beam tracking scheme and the 802.11ay beam tracking with different beamwidths for the given maximum beam angle offset ($\vartheta_{\max} = 180°$). With the increases of beamwidth, the overhead of the two beam tracking mechanisms ($N_{Fast,TRN}$ and $N_{802.11ay,TRN}$) decreases for the given beam angle offset (ϑ). We can reach the conclusion according to (15) and (16). However, when comparing the fast beam tracking with the 802.11ay beam tracking, it can be seen that the performance of the fast beam tracking is superior to that for 802.11ay. Furthermore, with the narrower beamwidth, the performance improvement is higher. The reason is that, with narrower beamwidth, there will be more beams needed to cover all directions. The overhead of the 802.11ay beam tracking will be higher since more beams need to be tracked. However, the overhead of the proposed fast beam tracking can be reduced by adjusting the beam tracking region based on the previous beam tracking results.

Since the moving directions of UAVs in the mmWave

This article has been accepted for publication in a future issue of this journal, but has not been fully edited. Content may change prior to final publication. Citation information: DOI 10.1109/TVT.2018.2890152, IEEE Transactions on Vehicular Technology

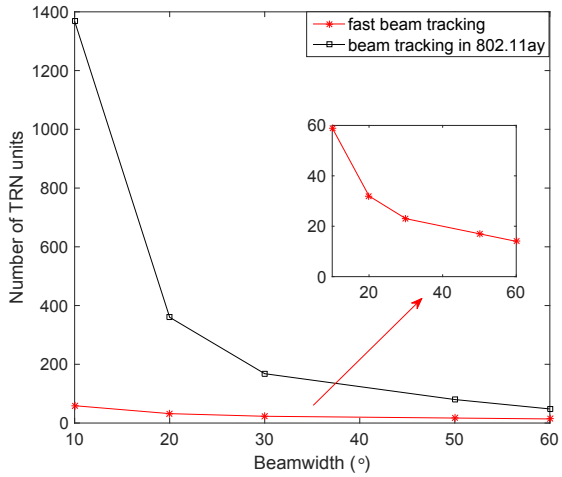

Fig. 8. The performance comparison between the fast beam tracking and 802.11ay beam tracking with different beamwidths.

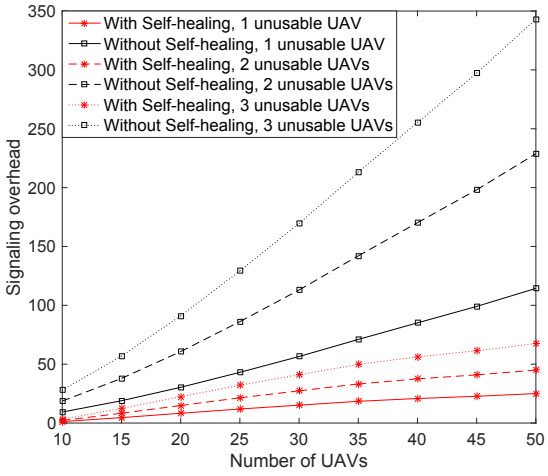

Fig. 9. The performance comparison between the proposed 'With Self-healing' mechanism and 'Without Self-healing' mechanism.

flyMesh are approximately the same (with proper platooning), which means that the relative moving speed between UAVs will be low. For the 802.11ay based mmWave networks, the channel bandwidth is 2.16 GHz and the subcarrier spacing is 5.15625 MHz [12], [13]. In order to analyze the influence of relative moving speed on beam tracking, we assume that the maximum relative moving speed between UAVs is 10 m/s. Then, according to (9), we can get the maximum Doppler shift is $f_{d,\max} = f_c \cdot v/c = 2000$ Hz. Then, $\mathrm{sinc}^2(f_{d,\max}T_s) = \mathrm{sinc}^2(f_{d,\max}/\Delta f) \approx 1$. According to (8), we obtain $P_{ICI} \approx 0$ with the most serious Doppler shift. Therefore, the influence of low relative moving speed on beam tracking can be ignored. The large subcarrier spacing plays an important role in combatting the Doppler shift.

B. The performance of self-healing mechanism

In order to find an alternative link to replace the unusable link, the time-consuming routing protocols in the network layer are not the good choices. In order to show the advantage of our proposed self-healing mechanism, we compare it with a MAC layer link recovery mechanism based on AODV protocol (named 'Without Self-healing' in Fig. 9) as described in Section III.B.

We consider the number of Self-healing Requests transmitted by UAVs for finding the forwarding link as the signaling overhead of self-healing. As shown in Fig. 9, with the increase of the number of UAVs in the mmWave flyMesh, the self-healing mechanism can reduce the signaling overhead significantly. According to Algorithm 2, we know that the signaling overhead of the self-healing mechanism is related to the average number of UAVs around each UAV and the steps between the upstream UAV of the unusable UAV and the downstream UAV of the unusable UAV. However, if self-healing is not adopted, the signaling overhead is related to the total number of UAVs in the mmWave flyMesh. We can see from Fig. 9 that the signaling overhead of the self-healing mechanism increases slowly with the increase of the number of UAVs. This is beacuse the average number of UAVs around each UAV increases with the increase of the number of UAVs in the mmWave flyMesh for the given network radius (500 m). Thus, the signaling overhead of self-healing will increase accordingly.

In addition, with the increases of the number of unusable UAVs, the signaling overhead increase significantly in both our proposed self-healing mechanism (i.e., 'With Self-healing' in Fig. 9) and the AODV protocol-based link recovery mechanism (i.e., 'Without Self-healing' in Fig. 9). For the traditional mechanism (i.e., Without Self-healing), the signaling overhead is directly proportional to the number of unusable UAVs. Similarly, more Self-healing Request frames and Self-healing Response frames should be transmitted to recover the mmWave flyMesh in our proposed self-healing mechanism when there are more unusable UAVs. We can also see from Fig. 9 that, the larger the number of unusable UAVs, the better the performance of our proposed self-healing mechanism. Because the searching area is limited just around the local area of unusable UAVs and other UAVs stop searching, and thus the signaling overhead can be reduced in our proposed self-healing mechanism.

Due to the low relative moving speed between UAVs, the fast beam tracking mechanism can ensure a stable connectivity between UAVs. It should be noted that, we only consider the signaling overhead of self-healing with stable connectivities between UAVs and there are no beamforming operations to be performed prior to the self-healing. Therefore, the relatively low moving speed between UAVs has negligible effect on the performance of the proposed self-healing mechanism.

C. The performance of efficient UAV group leader re-selection mechanism

Suppose the flight height of UAV is 100 m [4], the radius of the mmWave flyMesh is 500 m, and the other simulation parameters are shown in Table I. Fig. 10 shows the performance comparison on the number of candidate UAV group

leaders which perform beam training with rBS between the two UAV group leader re-selection mechanisms with different number of UAVs (i.e., from 10 to 50) and different beamwidths (i.e., 10°, 20°, 30°). The traditional UAV group leader re-selection mechanism in the 802.11ad/ay is based on the SINR between the candidate UAV group leader and rBS. However, the efficient UAV group leader re-selection mechanism as proposed in Section IV can limit the region of candidate UAV group leaders and thus reduce the number of UAV group leaders to perform beam training with rBS. That is the difference between the traditional and the efficient UAV group leader re-selection mechanism.

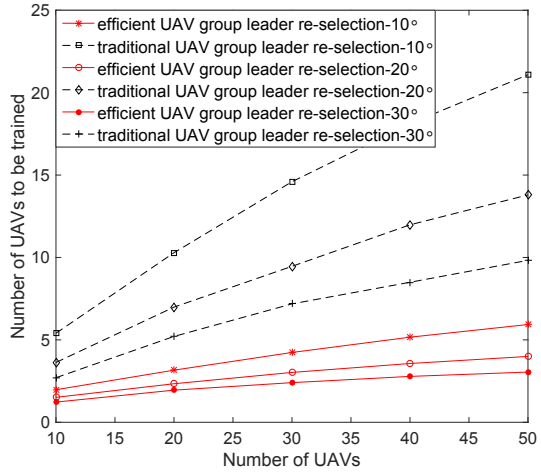

Fig. 10. The performance comparison on the number of UAVs to be trained between the two UAV group leader re-selection mechanisms with different beamwidths.

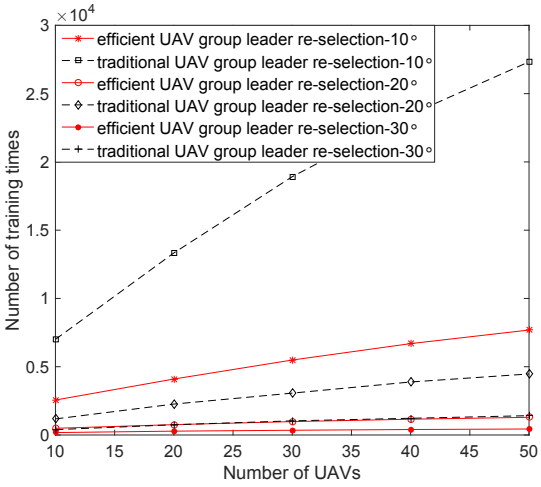

Fig. 11. The performance comparison on the number of training times between the two UAV group leader re-selection mechanisms with different beamwidths.

As shown in Fig. 10, the number of UAVs to be trained increases fast as the number of UAVs increases if the number of UAVs is small (e.g., less than 40). Since with small number of UAVs in the mmWave flyMesh, the interference is limited and the number of UAVs to be trained is determined by the total number of UAVs. However, when the number of UAVs is large (e.g., more than 50), the number of UAVs to be trained will slowly increase. This is because with the given mmWave flyMesh radius (500 m), if there are too many UAVs, the interference for each UAV will become worse according to (4) and [31]. Thus, the UAVs far away from the rBS will not be selected as the candidate UAV group leaders. Furthermore, Fig. 10 also shows that, the number of UAVs to be trained increases when the beamwidth decreases, since the SINR is higher with narrower beamwidth according to (5) and (6). Thus, the UAVs far away from rBS can still be selected as the candidate UAV group leaders. Fig. 11 shows the performance comparison on the number of beam training times between the two UAV group leader re-selection mechanisms with different number of UAVs (i.e., from 10 to 50) and different beamwidths (i.e., 10°, 20°, 30°). Since there are more beams to be trained with narrower beamwidth, we can see from Fig. 11 that the number of training times in the narrower beamwidth is larger than that of the wider beamwidth. Other observations for Fig. 11 are similar to those for Fig. 10.

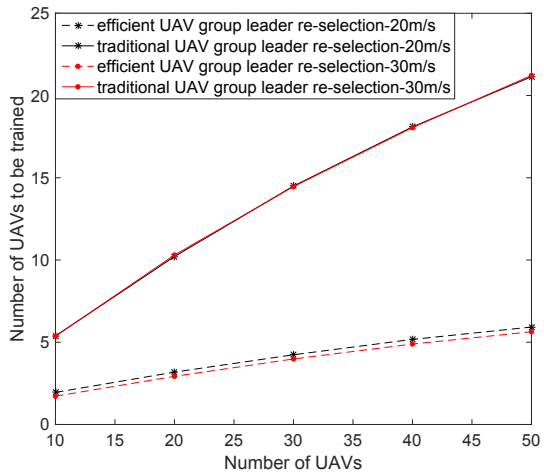

Fig. 12. The performance comparison on the number of UAVs to be trained between the two UAV group leader re-selection mechanisms with different flying speeds.

Since the relative moving speed between the UAV group leader and rBS (we assume the maximum relative moving speed is 30 m/s [1]) will be higher than the relative moving speed between two UAVs. Thus, we cannot ignore the Doppler shift between the UAV group leader and rBS. In order to analyze the effect of relative moving speed between the UAV group leader and rBS, we set the beamwidth to 10°. Fig. 12 and Fig. 13 show the number of candidate UAV group leaders needed to perform beam training with rBS and the number of beam training times when the flying speeds are 20 m/s and 30 m/s, respectively. As can be seen from Fig. 12 and Fig. 13 that, the number of UAVs to be trained and the corresponding beam training times for 30 m/s are almost the same with that of 20 m/s. That is to say, the small relative

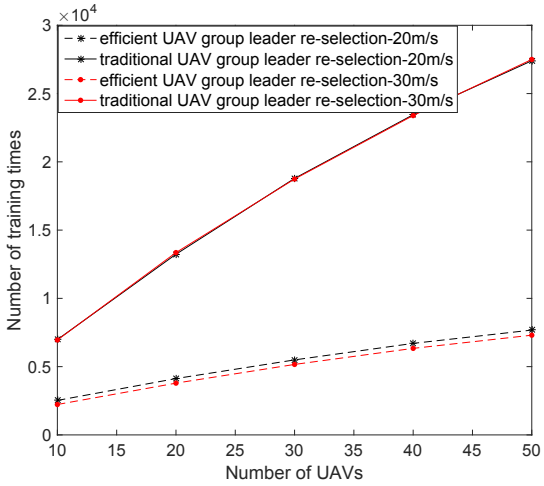

Fig. 13. The performance comparison on the number of training times between the two UAV group leader re-selection mechanisms with different flying speeds.

moving speed (up to 30 m/s) between the UAV group leader and rBS has little impact on the performance of UAV group leader re-selection. According to (8) and (11), we observe that, the higher the flying speed is, the larger the Doppler shift is and the smaller the SINR is. When determining the candidate UAV group leaders, there are fewer UAVs act as the candidate UAV group leader with higher flying speed. Therefore, with higher flying speed, the number of UAVs to be trained in Fig. 12 and the number of beam training times in Fig. 13 are a little bit smaller.

VI. Conclusions

The key challenges in designing mmWave flyMesh are mainly brought by the directional communications when compared with the microwave based flyMesh. The relative movement between UAVs or between the UAV group leader and relaying stations will result in beam misalignments. Unusability of UAV(s) due to mobility and power depletion will bring in frequent link failures in the mmWave flyMesh. To cope with the beam misalignments and link failures between UAVs, we have developed a fast beam traking mechanism. For the link failures caused by UAV unusability, we have designed a self-healing mechanism in MAC layer to repair the failed link in the mmWave flyMesh with low signaling overhead. Since flyMesh heavily rely on the UAV platooning, the choice of the UAV group leader (the coordinator) for both communications and control plays a significant role in effective network operations. Therefore, an efficient UAV group leader re-selection mechanism has been proposed to select a new UAV group leader whenever necessary due to mobility. These mechanisms have been shown to improve the robustness of the mmWave flyMesh and reduce the overhead in establishing the directional communication links, which also implies that the power is saved to extend the life time of UAVs. Performance analysis and extensive simulations studies have been carried out to show the effectiveness of the proposed mechanisms.

Appendix A
Proof of (15) and (16)

According to the beam pattern model in Section II, there are N_{test1} beams in $\mathbf{N}_i^{test1}$ and N_{test2} beams in $\mathbf{N}_i^{test2}$. When performing beam tracking, there are N_{test1} beams to be tracked in the first beam tracking step and N_{test2} beams to be tracked in the subsequent beam tracking steps. If the beam angle offset is ϑ and the beamwidth is α, there will be $\frac{\vartheta}{\alpha}$ steps needed for finding the optimal beam pair. Therefore, $N_{Fast,TRN} = N_{test1} + \left(\frac{\vartheta}{\alpha} - 1\right) \cdot N_{test2}$. However, for the beam tracking in 802.11ad/ay, taking the working beam as the center, it needs $\frac{\vartheta}{\alpha}$ rounds of beam tracking and contains $\left(2 \cdot \frac{\vartheta}{\alpha} + 1\right)^2$ beams to be tracked. Except for the working beam in the first round, the total number of beam tracking times is $N_{802.11ay,TRN} = \left(2 \cdot \frac{\vartheta}{\alpha} + 1\right)^2 - 1$. ■

Appendix B
Proof of (18)

When the upstream UAV of the unusable UAV searches for an alternative forwarding link, it transmits the Self-healing request to $n_{in,near} - 2$ UAVs (except the unusable UAV and its upstream UAV). The UAVs received the Self-healing request will continue transmitting the Self-healing request to $n_{in,near} - 1$ UAVs around themselves. Suppose we need s_{self} steps to find the downstream UAV of the unusable UAV to form the forwarding link, the signaling overhead can be expressed as

$$O_{self}{}' = \underbrace{(n_{in,near} - 2)}_{s_{self}=1} + \underbrace{(n_{in,near} - 2)(n_{in,near} - 1)}_{s_{self}=2} + \cdots + \underbrace{(n_{in,near} - 2)\underbrace{(n_{in,near} - 1)\cdots(n_{in,near} - 1)}_{s_{self}-1 \quad \text{items}}}_{s_{self}=s_{self}}. \tag{22}$$

According to the formula of summation for geometric sequence, we can rewrite (22) as

$$\begin{aligned} O_{self}{}' &= (n_{in,near} - 2) \cdot \frac{1 - (n_{in,near} - 1)^{s_{self}}}{1 - (n_{in,near} - 1)} \\ &= (n_{in,near} - 1)^{s_{self}} - 1. \end{aligned} \tag{23}$$

Since the above calculation does not consider the situation that part of the UAVs are on the edge of the mmWave flyMesh, and the neighboring UAVs for the UAVs on the edge of the mmWave flyMesh is fewer than that of the UAVs inside the mmWave flyMesh (i.e., $n_{out,near} < n_{in,near}$). Thus, we can get $O_{self} < O_{self}{}'$. ■

References

[1] J. Wang, C. Jiang, Z. Han, Y. Ren, R. G. Maunder and L. Hanzo, "Taking Drones to the Next Level: Cooperative Distributed Unmanned-Aerial-Vehicular Networks for Small and Mini Drones," *IEEE Veh. Technol. Mag.*, vol. 12, no. 3, pp. 73-82, Sep. 2017.

[2] L. Gupta, R. Jain and G. Vaszkun, "Survey of Important Issues in UAV Communication Networks," *IEEE Commun. Surv. Tuts.*, vol. 18, no. 2, pp. 1123-1152, Second Quarter 2016.

[3] Z. M. Fadlullah, D. Takaishi, H. Nishiyama, N. Kato and R. Miura, "A dynamic trajectory control algorithm for improving the communication throughput and delay in UAV-aided networks" *IEEE Netw.*, vol. 30, no. 1, pp. 100-105, Jan.-Feb. 2016.

[4] Y. Zeng, R. Zhang and T. J. Lim, "Wireless communications with unmanned aerial vehicles: opportunities and challenges," *IEEE Commun. Mag.*, vol. 54, no. 5, pp. 36-42, May 2016.

[5] F. Tang, Z. M. Fadlullah, N. Kato, F. Ono and R. Miura, "AC-POCA: Anticoordination Game Based Partially Overlapping Channels Assignment in Combined UAV and D2D-Based Networks," *IEEE Trans. Veh. Technol.*, vol. 67, no. 2, pp. 1672-1683, Feb. 2018.

[6] Z. Xiao, P. Xia and X. g. Xia, "Enabling UAV cellular with millimeter-wave communication: potentials and approaches," *IEEE Commun. Mag.*, vol. 54, no. 5, pp. 66-73, May 2016.

[7] Q. Xue, X. Fang, M. Xiao and L. Yan, "Multiuser Millimeter Wave Communications With Nonorthogonal Beams," *IEEE Trans. Veh. Technol.*, vol. 66, no. 7, pp. 5675-5688, Jul. 2017.

[8] M. Cheng, J. B. Wang, Y. Wu, X. G. Xia, K. K. Wong and M. Lin, "Coverage Analysis for Millimeter Wave Cellular Networks with Imperfect Beam Alignment," *IEEE Trans. Veh. Technol.*, vol. 67, no. 9, pp. 8302-8314, Sep. 2018.

[9] M. Xiao, S. Mumtaz, Y. Huang, *et al.*, "Millimeter Wave Communications for Future Mobile Networks," *IEEE J. Sel. Areas Commun.*, vol. 35, no. 9, pp. 1909-1935, Sep. 2017.

[10] X. Wu, C.-X. Wang, J. Sun, J. Huang, R. Feng, Y. Yang and X. Ge, "60-GHz Millimeter-Wave Channel Measurements and Modeling for Indoor Office Environments," *IEEE Trans. Antennas Propag.*, vol. 65, no. 4, pp. 1912-1924, Apr. 2017.

[11] X. Ge, R. Zi, X. Xiong, Q. Li and L. Wang, "Millimeter Wave Communications With OAM-SM Scheme for Future Mobile Networks," *IEEE J. Sel. Areas Commun.*, vol. 35, no. 9, pp. 2163-2177, Sep. 2017.

[12] *IEEE Standard for Information Technology - Telecommunications and information exchange between systems Local and metropolitan area networks - Specific requirements - Part 11: Wireless LAN Medium Access Control (MAC) and Physical Layer (PHY) Specifications*, IEEE Std 802.11-2016 (Revision of IEEE Std 802.11-2012), pp. 1-3534, Dec. 2016.

[13] *IEEE Draft Standard for Information Technology - Telecommunications and Information Exchange Between Systems Local and Metropolitan Area Networks - Specific Requirements - Part 11: Wireless LAN Medium Access Control (MAC) and Physical Layer (PHY) Specifications - Amendment 7: Enhanced throughput for operation in license-exempt bands above 45 GHz*, IEEE Std 802.11ay/Draft 1.0-2017, pp. 1-490, Nov. 2017.

[14] D. Takaishi, Y. Kawamoto, H. Nishiyama, N. Kato, F. Ono and R. Miura, "Virtual Cell Based Resource Allocation for Efficient Frequency Utilization in Unmanned Aircraft Systems," *IEEE Trans. Veh. Technol.*, vol. 67, no. 4, pp. 3495-3504, Apr. 2018.

[15] Q. Xue, X. Fang and C. X. Wang, "Beamspace SU-MIMO for Future Millimeter Wave Wireless Communications," *IEEE J. Sel. Areas Commun.*, vol. 35, no. 7, pp. 1564-1575, Jul. 2017.

[16] P. Zhou, X. Fang, Y. Fang, Y. Long, R. He and X. Han, "Enhanced Random Access and Beam Training for mmWave Wireless Local Networks with High User Density," *IEEE Trans. Wireless Commun.*, vol. 16, no. 12, pp. 7760-7773, Dec. 2017.

[17] P. Zhou, K. Cheng, X. Han, X. Fang, Y. Fang, R. He, Y. Long and Y. Liu, "IEEE 802.11ay based mmWave WLANs: Design Challenges and Solutions," *IEEE Commun. Surv. Tuts.*, vol. 20, no. 3, pp. 1654-1681, Third Quarter 2018.

[18] H. Ding, C. Zhang, Y. Cai and Y. Fang, "Smart Cities on Wheels: A Newly Emerging Vehicular Cognitive Capability Harvesting Network for Data Transportation," *IEEE Wireless Commun.*, vol. 25, no. 2, pp. 160-169, Apr. 2018.

[19] H. Ding, Y. Fang, X. Huang, M. Pan, P. Li and S. Glisic, "Cognitive Capacity Harvesting Networks: Architectural Evolution Toward Future Cognitive Radio Networks," *IEEE Commun. Surv. Tuts.*, vol. 19, no. 3, pp. 1902-1923, Third Quarter 2017.

[20] S. Imtiaz, G. S. Dahman, F. Rusek and F. Tufvesson, "On the directional reciprocity of uplink and downlink channels in Frequency Division Duplex systems," in *Proc. IEEE 25th Annu. Int. Symp. Pers., Indoor, and Mobile Radio Commun. (PIMRC)*, pp. 172-176, Sep. 2014.

[21] T. Bai and R. W. Heath, "Coverage and rate analysis for millimeter-wave cellular networks," *IEEE Trans. Wireless Commun.*, vol. 14, no. 2, pp. 1100-1114, Feb. 2015.

[22] A. Ancora, I. Toufik, A. Bury and D. Slock, "Orthogonal Frequency Division Multiple Access (OFDMA)," in *LTE - The UMTS Long Term Evolution: From Theory to Practice*, 2nd ed. New York, NY, USA: Wiley, 2009, ch. 5, sec. 5.2.3, pp. 165-167.

[23] A. Alkhateeb, Y. H. Nam, M. S. Rahman, J. Zhang and R. W. Heath, "Initial Beam Association in Millimeter Wave Cellular Systems: Analysis and Design Insights," *IEEE Trans. Wireless Commun.*, vol. 16, no. 5, pp. 2807-2821, May 2017.

[24] Y. Cai, F. R. Yu, J. Li, Y. Zhou and L. Lamont, "Medium Access Control for Unmanned Aerial Vehicle (UAV) Ad-Hoc Networks With Full-Duplex Radios and Multipacket Reception Capability," *IEEE Trans. Veh. Technol.*, vol. 62, no. 1, pp. 390-394, Jan. 2013.

[25] A. Iwata, C. Chiang, G. Pei, M. Gerla and T. Chen, "Scalable routing strategies for ad hoc wireless networks," *IEEE J. Sel. Areas Commun.*, vol. 17, no. 8, pp. 1369-1379, Aug. 1999.

[26] W. Liu, C. Zhang, G. Yao and Y. Fang, "DELAR: A Device-Energy-Load Aware Relaying Framework for Heterogeneous Mobile Ad Hoc Networks," *IEEE J. Sel. Areas Commun.*, vol. 29, no. 8, pp. 1572-1584, Sep. 2011.

[27] X. Huang, H. Zhai and Y. Fang, "Robust cooperative routing protocol in mobile wireless sensor networks," *IEEE Trans. Wireless Commun.*, vol. 7, no. 12, pp. 5278-5285, Dec. 2008.

[28] C. Perkins, E. Belding-Royer and S. Das, "Ad hoc On-Demand Distance Vector (AODV) Routing", RFC 3561, doi:10.17487/RFC3561, Jul. 2003. [Online]. Available: https://www.rfc-editor.org/info/rfc3561.

[29] A. K. Sadek, Z. Han and K. J. Ray Liu, "A Distributed Relay-Assignment Algorithm for Cooperative Communications in Wireless Networks," in *Proc. IEEE Int. Conf. Commun. (ICC)*, pp. 1592-1597, Jun. 2006.

[30] Y. Sun, X. Wang, D. Shen, M. Wu, N. Bao, T. Song and L. Shen, "Goodput performance of ultrahigh-speed WLAN via link adaptation algorithm," in *Proc. IEEE 12th Int. Conf. Commun. Technol. (ICCT)*, pp. 1344-1348, Nov. 2010.

[31] X. Yuan, Z. Feng, W. Xu, W. Ni, A. Zhang, Z. Wei and R.-P. Liu, "Capacity Analysis of UAV Communications: Cases of Random Trajectories," *IEEE Trans. Veh. Technol.*, vol. 67, no. 8, pp. 7564-7576, Aug. 2018.

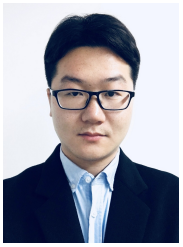

Pei Zhou received the B.E. degree in communication engineering from Southwest Jiaotong University, Chengdu, China, in 2015. He is currently working toward the Ph.D. degree with the Key Laboratory of Information Coding and Transmission, School of Information Science and Technology, Southwest Jiaotong University, Chengdu, China. His research interests include radio resource management for mmWave wireless networks, machine learning, etc.

Xuming Fang (M'00-SM'16) received the B.E. degree in electrical engineering in 1984, the M.E. degree in computer engineering in 1989, and the Ph.D. degree in communication engineering in 1999 from Southwest Jiaotong University, Chengdu, China. He was a Faculty Member with the Department of Electrical Engineering, Tongji University, Shanghai, China, in September 1984. He then joined the School of Information Science and Technology, Southwest Jiaotong University, Chengdu, where he has been a Professor since 2001, and the Chair of the Department of Communication Engineering since 2006. He held visiting positions with the Institute of Railway Technology, Technical University at Berlin, Berlin, Germany, in 1998 and 1999, and with the Center for Advanced Telecommunication Systems and Services, University of Texas at Dallas, Richardson, in 2000 and 2001. He has, to his credit, around 200 high-quality research papers in journals and conference publications. He has authored or coauthored five books or textbooks. His research interests include wireless broadband access control, radio resource management, multihop relay networks, and broadband wireless access for high speed railway. Dr. Fang is the Chair of the IEEE Vehicular Technology Society of Chengdu Chapter, and an Editor of the IEEE TRANSACTIONS ON VEHICULAR TECHNOLOGY.

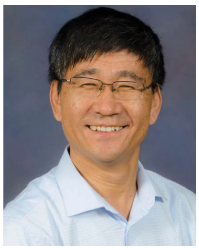

Yuguang Fang (F'08) received an MS degree from Qufu Normal University, Shandong, China in 1987, a PhD degree from Case Western Reserve University in 1994, and a PhD degree from Boston University in 1997. He joined the Department of Electrical and Computer Engineering at University of Florida in 2000 and has been a full professor since 2005. He holds a University of Florida Research Foundation (UFRF) Professorship (2017-2020, 2006-2009), University of Florida Term Professorship (2017-2019), a Changjiang Scholar Chair Professorship (Xidian University, Xi'an, China, 2008-2011; Dalian Maritime University, Dalian, China, 2015-2018), and Overseas Academic Master (Dalian University of Technology, Dalian, China, 2016-2018).

Dr. Fang received the US National Science Foundation Career Award in 2001, the Office of Naval Research Young Investigator Award in 2002, the 2015 IEEE Communications Society CISTC Technical Recognition Award, the 2014 IEEE Communications Society WTC Recognition Award, and the Best Paper Award from IEEE ICNP (2006). He has also received a 2010-2011 UF Doctoral Dissertation Advisor/Mentoring Award, a 2011 Florida Blue Key/UF Homecoming Distinguished Faculty Award, and the 2009 UF College of Engineering Faculty Mentoring Award. He was the Editor-in-Chief of IEEE TRANSACTIONS ON VEHICULAR TECHNOLOGY (2013-2017), the Editor-in-Chief of IEEE WIRELESS COMMUNICATIONS (2009-2012), and serves/served on several editorial boards of journals including IEEE TRANSACTIONS ON MOBILE COMPUTING (2003-2008, 2011-2016), IEEE TRANSACTIONS ON COMMUNICATIONS (2000-2011), and IEEE TRANSACTIONS ON WIRELESS COMMUNICATIONS (2002-2009). He has been actively participating in conference organizations such as serving as the Technical Program Co-Chair for IEEE INFOCOM'2014 and the Technical Program Vice-Chair for IEEE INFOCOM'2005. He is a fellow of the IEEE and a fellow of the American Association for the Advancement of Science (AAAS).

Rong He received the B.E. degree in automation control in 1997, the M.E. degree in Communication Information Engineering and Control in 2002, and the Ph.D. degree in computer application technology in 2011 from Southwest Jiaotong University, Chengdu, China. In 1997, she joined the School of Information Science and Technology, Southwest Jiaotong University, where she has been an associated professor since 2009. She held visiting position with the Department of Electrical and Computer Engineering, University of Waterloo, Ontario, Canada, from 2014 to 2015. She has published more than 30 research papers in journals and conferences. Her research interests include wireless broadband access control, radio resource management, next generation Wi-Fi.

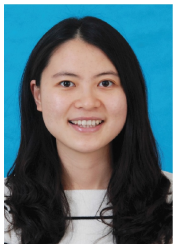

Yan Long (M'16) is currently a lecturer at School of Information Science and Technology, Southwest Jiaotong University, Chengdu, China. She received B.E. degree in Electrical and Information Engineering in 2009, and Ph.D. degree in Communication and Information Systems in 2015 from Xidian University, Xi'an, China. From September 2011 to March 2013, she was a visiting student in the Department of Electrical and Computer Engineering, University of Florida, USA. Her research interests include millimeter wave wireless communications, internet of things, 5G cellular networks, cognitive radio networks and wireless resource optimization.

Gaoyong Huang received the B.E. degree in Communication Engineering in 2003, the M.E. degree in Computer Application Technology in 2006, and the Ph.D. degree in Communication and Information System in 2014 from Southwest Jiaotong University, Chengdu, China. In 2006, he joined the School of Information Science and Technology, Southwest Jiaotong University, where he has been a lecturer since 2008. His research interests include radio resource management, 5G cellular networks, wireless Communication in Rail Transit.